Taylor dispersion analysis using capacitively coupled contactless conductivity detector

Chutintorn Somnin, Joseph Chamieh, Phoonthawee Saetear, Hervé Cottet

Taylor Dispersion Analysis Using Capacitively Coupled Contactless Conductivity Detector

Chutintorn Somnin[1], Joseph Chamieh[1], Phoonthawee Saetear[2,3*], Hervé Cottet[1*]

[1] IBMM, Université de Montpellier, CNRS, ENSCM, Montpellier, France

[2] Flow Innovation-Research for Science and Technology Laboratories (Firstlabs), Ratchathewi District, Bangkok 10110, Thailand

[3] Department of Chemistry and Center of Excellence for Innovation in Chemistry, Faculty of Science, Mahidol University, Rama 6 Road, Ratchathewi District, Bangkok 10400, Thailand

[*]E-mail address's corresponding authors: herve.cottet@umontpellier.fr (Prof. Hervé Cottet); phoonthawee.sae@mahidol.edu (Asst. Prof. Phoonthawee Saetear)

ABSTRACT

Taylor dispersion analysis (TDA) is a simple and absolute method to determine the hydrodynamic radius of solutes that respond to UV or fluorescence detections. To broaden the application range of TDA, it is necessary to develop new detection modes. This study aims to study capacitively coupled contactless conductivity detector (C^4D) for the analysis of charged macromolecules. The detection sensitivities and hydrodynamic radii were compared for a C^4D detector and a UV detector on positively or negatively charged polymers responding both to UV and C^4D (poly-L-lysine and poly(acrylamide-co-2-acrylamido-1-methyl-propanesulfonate). The influence of the composition of the background electrolyte on the detection sensitivity has been studied and optimized for C^4D detection. The influence of the molar mass and of the polymer chemical charge density on the C^4D and UV sensitivities of detection have been investigated based on well-characterized copolymers samples of different molar masses and charge densities. The advantages and disadvantages compared to UV detection, as well as the range of applicability of C^4D detection in TDA were identified. C^4D detection can be an alternative method for sizing charged polymers of reasonable molar mass (typically below 10^5 g mol^{-1}) that do not absorb in UV. A decline in the sensitivity of detection in C^4D was observed for higher molar masses.

Keywords: Taylor dispersion analysis, contactless capacitively coupled conductivity detection, polyelectrolytes, size-based characterization

1. Introduction

Taylor dispersion analysis (TDA) is an absolute method (no calibration needed) allowing the determination of the molecular diffusion coefficient (D), and of the hydrodynamic radius (R_h) of solutes of virtually any size in the range of 0.1-200 nm [1,2]. It can be applied to synthetic and biopolymers (such as proteins or polysaccharides) [3, 4], nanoparticles or colloids [5], and nanogels [6]. TDA is based on the dispersion of an injected band under a laminar Poiseuille flow. Its implementation in narrow bore capillaries (typically ~50 µm i.d.) presents several advantages, such as a low sample consumption (a few nL), a short analysis time, a wide range of sizing and straightforward analysis, without any sample preparation or filtration. Recently, it has been demonstrated that it is possible to retrieve from TDA data the full-size distribution of polydisperse samples (hydrodynamic radius or diffusion coefficient distributions) via an adequate data processing of the taylorgrams (called Constrained Regularized Linear Inversion) [7]. This makes this method particularly attractive, especially for the characterization of ultra-small nanoscale objects (< 10 nm), for which alternative sizing methods (such as dynamic light scattering) are limited by the weak signal. Moreover, TDA affords the determination of the mass-weighted distribution of the hydrodynamic radius in solution for mass-sensitive detector (as opposed to square mass-weighted for light scattering), has low sensitivity to dust, and can be performed under conditions close to those of real-life applications [8]. One limitation of TDA is the detection mode, which is limited to UV (or fluorescent) detections when performed on commercial Capillary Electrophoresis (CE) instrumentations. The development of alternative detections modes that can be used online with microscale capillaries is a key point to extent the field of applications of TDA to non-UV responding or non-fluorescent solutes. Non-UV absorbing polysaccharides can be detected by photochemical oxidation [3] but the sensitivity is relatively low with limited linear and dynamic ranges. Backscattering interferometry detection can also be used as a universal detection mode sensitive to changes in refractive index [9]. However, this detection mode lakes robustness relative to temperature changes and required a specific optical bench with adequate optical adjustment.

A capacitively coupled contactless conductivity detector (C^4D) is a detector measuring the conductivity of the electrolyte passing through the detector without physical contact between the electrolyte and the electrodes. This avoids electrode passivation. Various terminologies have been used to describe C^4D principle, e.g., impedance sensor [10-13], oscillometric detector [14-17], and admittance detector [18-20]. C^4D detection is relatively popular in CE [21,22], especially for the detection of small ions or underivatized amino acids including for clinical studies [23, 24]. Its application to the detection of charged polymers [25] or nanoparticles has been much less investigated in CE. To our knowledge, at that date, no article using C^4D as a detector in TDA (all solutes considered) was published. The use of conductivity detectors in liquid chromatography is generally assumed to be restricted to charged ions or to charged polymers in a conductive eluent (typically water-based electrolyte) [26]. However, Oudhoff *et al.* demonstrated that C^4D could also be used for the detection of neutral polymers in non-aqueous capillary size-exclusion electrochromatography [27] and mentioned that this detection mode appeared as an interesting alternative for non-UV absorbing macromolecules in microcapillary format (for which other detection modes such as refractive index, are not available). Even if the origin of the C^4D response in the case of neutral polymers was not clearly understood and

was not related to the change in viscosity associated to the polymer sample zone [27], C^4D appears as a powerful versatile and universal detection mode for TDA applications in narrow bore capillaries.

In this work, for the first time, we aimed to investigate the use of C^4D for the size-characterization of charged polymers by TDA. For that, we first investigated the use of C^4D on UV-absorbing anionic and cationic polyelectrolytes to better understand how the C^4D detector response changes with the solute characteristics (molar mass and chemical charge density). To better compare the two detection modes, simultaneous detection modes were performed in the same TDA run using a series of well-defined copolymer samples of various charges and various molar masses. Finally, C^4D-TDA was successfully applied to a non-UV absorbing polyelectrolyte.

2. Material and methods

2.1 Chemicals

The chemical structures of polyelectrolytes and their characteristics (average molar mass, nominal charge density and polydispersity index) were listed in Fig. SI-1 and Table SI-1. Poly (L-lysines) (PLL) under their chloride form at different degree of polymerization (DP): PLL20, PLL50, PLL100, PLL250 and PLL400, were provided from Alamanda Polymers (Huntsville, AL). Poly(acrylamide-co-2-acrylamido-1-methyl-propanesulfonate) (SPAM) and poly(acrylic acid-co-acrylamide) (APAM) of different molar masses were kindly provided by SNF SA (Andrézieux, France). Poly(acrylic acid) (PAA) M_n = 3.7x10^4 g mol^{-1} was from Polymer sources (Canada). Polydiallyldimethylammonium chloride (PDADMAC) 20%, M = 4–5x10^5 g mol^{-1} was purchased from Sigma-Aldrich (Saint Quentin Fallavier, France).

β-alanine, histidine, 4-morpholinepropanesulfonic acid (MOPS), tris(hydroxymethyl)aminomethane (Tris), and sodium tetraborate decahydrate were from Sigma-Aldrich (Saint Quentin Fallavier, France). Sodium hydroxide and acetic acid were from BDH chemicals (VMR, Paris, France). Hydrochloric acid and formic acid were from Fluka (Illkirch, France) and 2,2-Bis(hydroxymethyl)-2,2',2''-nitrilotriethanol (Bis-tris) was purchased from Acros Organics (Geel, Belgium). All the electrolytes and buffer solutions were prepared using ultrapure water purified with a Milli-Q system from Millipore (Molsheim, France).

2.2 Taylor Dispersion Analysis

2.2.1 Experimental protocol

All TDA experiments were performed on a 7100 CE Agilent system (Waldbronn, Germany). This system was coupled with a C^4D detector from Tracedec® (Strasshof an der Nordbahn, Austria) and a built-in UV detector. Bare fused-silica capillary (Polymicro technologies, USA) of 50 µm i.d. and 360 µm o.d. with a total length of 60 cm was used and inserted in the C^4D head which is placed in the cassette as shown in Fig 1. The position of the C^4D head and UV detection window are 46.4 and 51.5 cm from the inlet side, respectively, which allowed for simultaneous detection from both detectors. C^4D detection was performed without removing the polyimide coating, but UV detection necessitates the removal of the polyimide layer in order to achieve UV transparency.

The principle of C^{4}D detection is shown on the right-hand side of the diagram in Fig. 1 and has been fully described elsewhere [28-32]. Briefly, the C^{4}D detector is made of two electrodes, which are placed cylindrically around the capillary tube with a small gap between the electrodes and are connected to an AC oscillator. The measured signal is proportional to the change in conductivity when an analyte zone with a different conductivity from that of the BGE passes the detection gap. For Tracedec® C^{4}D instrumentation, different parameter settings (frequency, voltage, gain and offset) affect the output signal and were optimized to get the best signal to noise ratio. In this work, the voltage was set at the maximum value (0 dB). The gain was set at the maximum value without saturation of the signal (50% or 75% depending on the conductivity of the buffer).

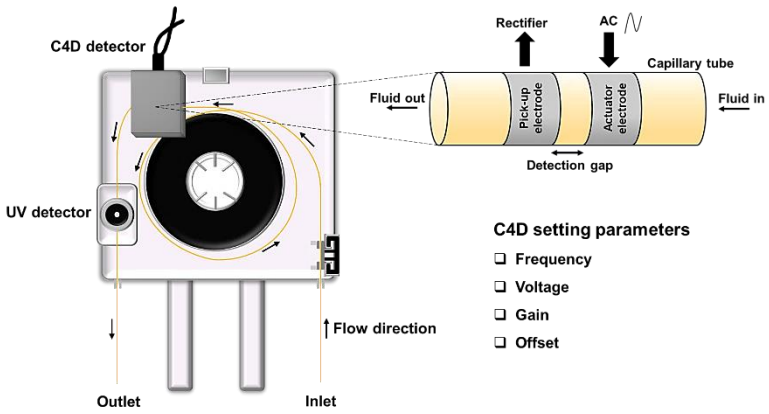

Fig. 1. Schematic diagram of capillary setup for Taylor dispersion analysis with C^{4}D and UV detector and the composition of an axial C^{4}D system. The capillary cassette represented in this Figure is used with the Agilent 7100 apparatus.

In the case of the analysis of polyanions by TDA, new capillaries were conditioned with the following flushes: 1 M NaOH for 30 min, water for 15 min and buffer for 15 min. In the case of polycation analysis, the inner surface of the capillary was modified by flushing a PDADMAC 0.2% m:m in water to avoid the interaction between the polymer sample and the capillary surface. The coating procedure is based on a previously published protocol [33] as follows: 1 M NaOH for 30 min; water for 15 min; PDADMAC 0.2% m:m in water for 30 min; water for 15 min and buffer for 15 min. Samples were injected hydrodynamically on the inlet side of the capillary (20 mbar, 10 s) for online detection by both detectors (V_i/V_d < 1%), where V_i/V_d is the ratio of the injected sample volume to the volume of capillary from inlet to the closest detector. TDA was performed using a mobilization pressure of 100 mbar. Between each run, the capillary was rinsed by flushing with water for 5 min and then with buffer for 5 min. All experiments were carried out at 25 ºC.

2.2.2 Theoretical aspects

Briefly, TDA is based on the mobilization of a sample plug in an open capillary tube under a laminar Poiseuille flow. The parabolic velocity profile of the Poiseuille flow combined to the molecular diffusion which redistributes the solutes along the tube's section, results in the so-called Taylor dispersion. For a single size sample mixture, the elution profiles recorded at the detection points are Gaussian shape [1, 2]. The band broadening resulting from Taylor dispersion is related to the temporal variance of the elution profile, σ^2 (in s^2) which can be quantified by Gaussian fitting in the case of a

monodisperse sample, or by peak integration in the case of a polydisperse sample. The average molecular diffusion coefficient, D (m^2 s^{-1}) of the solutes can be calculated using Equation (1) and transformed into the hydrodynamic radius R_h (m) using the Stokes Einstein equation (Equation (2)):

$$D = \frac{R_c^2 t_0}{24\sigma^2} \quad (1)$$

$$R_h = \frac{k_B T}{6\pi\eta D} \quad (2)$$

where R_c is the capillary radius (m), t_0 is the average elution time (s), k_B is the Boltzmann constant (Pa m^3 K^{-1}), T the temperature (K) and η the viscosity of the carrier liquid (Pa s). Equation (1) is valid when two conditions are fulfilled. First, t_0 should be much higher than the characteristic diffusion time of the solute in the cross section of the capillary, *i.e.* $t_0 \geq 1.25\ R_c^2/D$ for a relative error (ε) on the determination of D lower than 3%. Second, the axial diffusion should be negligible as compared to convection (*i.e.* when the Péclet number $Pe = \frac{R_c u}{D}$ is higher than 40 for (ε) lower than 3%, where u is the linear velocity (m s^{-1}) [34]).

In this study, a lab-made Excel spreadsheet was used for data processing of taylorgrams, including the fitting of the elution profile by a sum of Gaussian peaks using Excel solver and the determination of the temporal variance of the polymer contribution. The multi-gaussian fitting (up to 3) allows to subtract the small ion contribution before integration of the polymer contribution to get the average diffusion coefficient and hydrodynamic radius.

3. Results and discussions

3.1 Effect of applied frequency on the C^{4}D signal

In this study, we have first optimized the applied frequency of the C^{4}D detector on the polymer response. In C^{4}D detection the frequency supplied to the cell has a significant impact on the performance of the detector [35, 36]. In order to obtain the highest response, the applied frequency was therefore varied using the available frequencies from the Tracdec® instrument which were noted as medium, high, and 2x high. The other operating parameters such as the gain and the offset were set constant and are indicated in the figure caption. In the case of polyanion analysis, SPAM A3 was selected to study this parameter using 100 mM histidine pH 7.68 as the mobile phase, as shown in Fig. 2A. When the medium frequency was applied, the polymer could not be detected and the signal showed a taylorgram corresponding to the small ions which are present as impurities in the polymer solution. These small ions contribution can be reduced by doing dialysis against BGE without affecting the calculated R_h of the polymer (see Fig. SI-2). When a higher frequency was applied, the polymer could be detected as a broad peak even if the small ion contribution also increased in intensity. Similar results were obtained for polycation analysis (PLL100 in 8 mM Tris-Cl pH 7.4), as shown in Fig. 2B. The frequency at 2x high gave the highest C^{4}D signals and was therefore chosen as the working frequency for the analysis of both polyanions and polycations.

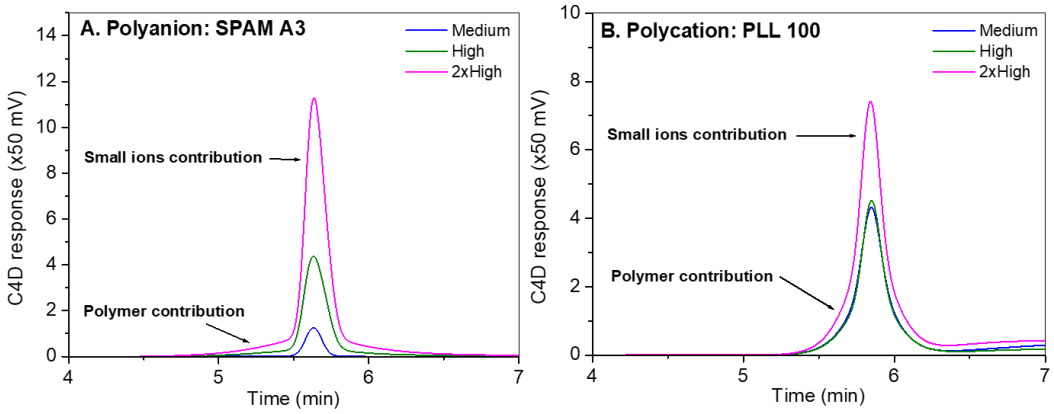

Fig. 2. Taylorgrams with C^{4}D detection of polyanion SPAM A3 (A) and polycation, PLL 100 (B) at different C^{4}D applied frequency. Experimental conditions for polyanion: fused silica capillary of 60 cm total length (46.4 cm to C^{4}D detector, 51.5 cm to UV detector) x 50 µm i.d. Eluent: 100 mM histidine (pH 7.68, ionic strength 2.276 mM, conductivity 114 µS cm^{-1}). Capillary preconditioning: Flush with water for 2 min followed by BGE for 3 min. Sample injection: 20 mbar, 10 s (0.6% of the capillary volume to the detector). Polymer samples: all polymers at 5.0 g L^{-1} in the eluent. Mobilization pressure: 100 mbar. C^{4}D parameters: Blue line; frequency: medium, voltage: 0 dB, gain: 75%, offset: 0, Green line; frequency: high, voltage: 0 dB, gain: 75%, offset: 0, Pink line; frequency: 2x high, voltage: 0 dB, gain: 75%, offset: 0. Experimental conditions for polycation: PDADMAC coated capillary, 60 cm total length (46.4 cm to C^{4}D detector, 51.5 cm to UV detector) x 50 µm i.d. Eluent: 8 mM Tris-Cl (pH 7.4, ionic strength 6.7 mM, conductivity 661 µS cm^{-1}). Capillary preconditioning: flushing DI for 2 min followed by BGE for 3 min. Injection: 20 mbar, 10 s (0.6% of the capillary volume to the detector). Mobilization pressure: 100 mbar. C^{4}D parameters: Blue line; frequency: medium, voltage: 0 dB, gain: 50%, offset: 20, Green line; frequency: high, voltage: 0 dB, gain: 50%, offset: 20, Pink line; frequency: 2xhigh, voltage: 0 dB, gain: 50%, offset: 20.

3.2 Effect of the background electrolyte

The background electrolyte (BGE) is also an important parameter which can affect the detector response, the noise and the peak profile. It is worth noting that the C^{4}D response in TDA is not the same as the one obtained in CE due to the absence of electric field in TDA. The C^{4}D response is expected to be directly related to the change in conductivity between the polymer zone and the BGE zone. For an injected polymer solution having the BGE as a matrix, it could be theoretically expected that the BGE conductivity is only impacting the background conductivity signal and not the polymer response itself. Various BGE compositions (6 BGE for polyanions, and 3 BGE for polycations) were tested with all details about their compositions given in Table SI-2. The choice of the BGE has been performed based on typical buffer used in C^{4}D for CE (*e.g.* histidine or acetic acid) or the well-known low conductive buffers (also called the goods buffers, such as MOPS) or in UV-CE (*e.g.* sodium borate or TRIS-Cl buffers). The signal profiles obtained for SPAM A10 polyanion are displayed in Fig. 3. The 20 mM sodium borate pH 9.2 and the 10 mM MOPS sodium pH 7.2 buffers provided the highest signal for the polymer with a symmetrical peak shape in both C^{4}D and UV detectors. Sodium MOPS was retained for the rest of the study for polyanion analysis because of the lower LOD compared to sodium borate buffer (0.10 g L^{-1} versus 0.27 g L^{-1} for SPAM A10). We can also notice that the signal contribution of the small ions is more important in C^{4}D than in UV, relatively to the charged polymer contribution (see Fig. 3). As for polycation analysis, the BGE that gave the highest response for PLL (DP 250) with a symmetrical peak shape was 8 mM Tris-Cl buffer pH 7.4, as shown in Fig. 4.

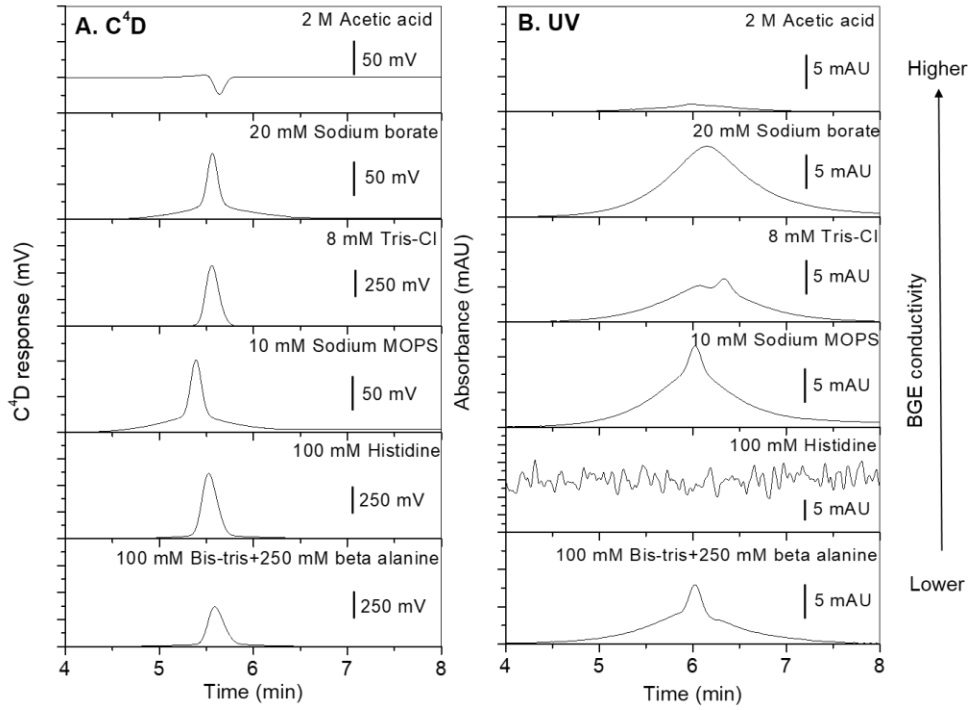

Fig. 3. Taylorgrams of SPAM A10 in different BGE with C^4D (A) and UV (B) detections. Experimental conditions: fused silica capillary of 60 cm total length (46.4 cm to C^4D detector, 51.5 cm to UV detector) x 50 µm i.d. Eluent: as indicated in each figure. Mobilization pressure: 100 mbar. Capillary preconditioning: Flush with water for 2 min followed by BGE for 3 min. Sample injection: 20 mbar, 10 s (0.6% of the capillary volume to the closest detector). Sample: SPAM A10 at 5.0 g L^{-1} in the eluent. UV detection at 200 nm at 25ºC. C^4D parameters: Acetic acid as BGE, frequency: 2x high, voltage: 0 dB, gain: 50%, offset: 100. Sodium borate as BGE, frequency: 2x high, voltage: 0 dB, gain: 50%, offset: 40. Tris-Cl as BGE, frequency: 2x high, voltage: 0 dB, gain: 50%, offset: 30. MOPS sodium as BGE, frequency: 2x high, voltage: 0 dB, gain: 50%, offset: 25. Histidine as BGE, frequency: 2x high, voltage: 0 dB, gain: 50%, offset: 5. Bis-tris+β-alanine as BGE, frequency: 2x high, voltage: 0 dB, gain: 50%, offset: 5.

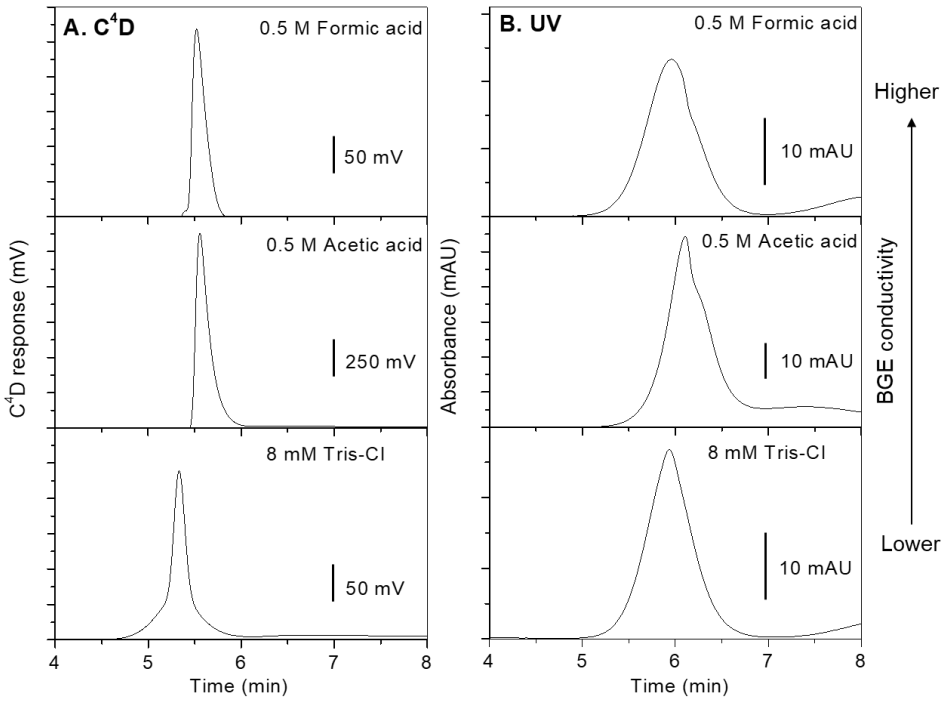

Fig. 4. Taylorgrams of PLL250 in different BGE with C^{4}D (A) and UV (B) detections. Experimental conditions: PDADMAC coated capillary, 60 cm total length (46.4 cm to C^{4}D detector, 51.5 cm to UV detector) x 50 µm i.d. Eluent: as indicated in each figure. Mobilization pressure: 100 mbar. Capillary preconditioning: Flush with water for 2 min followed by BGE for 3 min. Injection: 20 mbar, 10 s (0.6% of the capillary volume to the closest detector). Sample: PLL250 at 3.0 g L^{-1} in the eluent. UV detection at 200 nm at 25ºC. C^{4}D parameters: Formic acid as BGE, frequency: 2xhigh, voltage: 0 dB, gain: 50%, offset: 170. Acetic acid as BGE, frequency: 2xhigh, voltage: 0 dB, gain: 50%, offset: 75. Tris-Cl as BGE, frequency: 2xhigh, voltage: 0 dB, gain: 50%, offset: 35.

3.3 Effect of polyelectrolyte charge density on C^{4}D response

Fig. 5 displays the variation in the C^{4}D and UV responses as a function of the chemical charge density *f* for the SPAM family at constant injected mass concentration. *f* is defined as the molar content of sulfonated monomer in the SPAM polymer and was varied from 10% to 100%. It should be noted that, as expected, no signal could be detected with the polyacrylamide (*f*=0), due to the lack of charge/conductivity of the polymer. All the corresponding taylorgrams are gathered in Fig. SI-3. Fig. 5A clearly shows that the C4D response first increases linearly with *f* before levelling off. On the contrary, in UV detection (Fig. 5B), the signal almost remains constant on the whole *f* range. The UV response relative to the mass concentration depends on both the absorbance of the amide and the sulfonated functional groups. The charged repeating unit should absorb more than the neutral one but since the charged repeating unit also weighs more than the neutral one, both effects should compensate, at least partially. To better explain the C^{4}D response, it is necessary to express the conductivity signal as the difference in conductivity between the eluent and the polymer zone. This difference in conductivity corresponds to the conductivity of the polymer chain $\kappa_{\text{polymer chain}}$ including the contribution of the polymer counterions $\kappa_{\text{polymer counterions}}$:

$$\Delta\kappa = \kappa_{polymer\ zone} - \kappa_{BGE} = \kappa_{polymer\ chain} + \kappa_{polymer\ counterions} \quad (3)$$

The conductivity κ_i (in S m^{-1}) of a given charged specie *i* is related to its electrophoretic mobility μ_i (in m^2 V^{-1} s^{-1}), its effective charge z_i, its molar concentration C_i (in mol L^{-1}) and the Faraday constant F (in C mol^{-1}) according to eq. (4):

$$\kappa_i = \mathrm{F}\, c_i\, z_i \mu_i \quad (4)$$

The molar concentration in charged monomer $C_{M,1}$ (sulfonated repeating unit) in the sample zone is related to the mass polymer concentration $C_{m,\,polymer}$ according to:

$$c_{\mathrm{M},1} = \frac{C_{m,\,polymer}\, f}{f M_1 + (1-f)\,\mathrm{M}_2} \quad (5)$$

where M_1 is the molar mass of a charged repeating unit (g mol^{-1}), and M_2 is the molar mass of the uncharged repeating unit (g mol^{-1}). The molar concentration in polymer counter-ion is equal to $C_{M,1}$ leading to eq. (6) by combining equations (3) to (4):

$$\Delta\kappa = (\mu_{polymer\ chain} + \mu_{polymer\ counterions})\,\mathrm{F}\, c_{M,1}\, z_1 \quad (6)$$

where $\mu_{polymer\ chain}$ is the effective electrophoretic mobility of the polymer chain, $\mu_{polymer\ counterons}$ is the effective electrophoretic mobility of the counterions. Two regimes should be distinguished: below and above the Manning counterion condensation threshold [37]. Below the condensation threshold, corresponding to f =37% for a vinylic polyelectrolyte, all the charged repeating units bare one nominal charge (z_1=-1) and are completely dissociated from their counterions. Above the counterion condensation threshold, counterion condensation occurs and the effective charge per sulfonate group z_1 decrease with f according to:

$$z_1 = \frac{0.37}{f} \tag{7}$$

Therefore, the difference in conductivity is expressed as:

$$\Delta\kappa = (\mu_{polymer\,chain} + \mu_{polymer\,counterions})\,\mathrm{F}\,c_{M,1} \qquad \text{for } f < 0.37 \tag{8}$$

$$\Delta\kappa = (\mu_{polymer\,chain} + \mu_{polymer\,counterions})\,\mathrm{F}\,c_{M,1} \times \frac{0.37}{f} \qquad \text{for } f > 0.37 \tag{9}$$

Finally, equations (8) and (9) were plotted in solid line in Fig. 5A taking $\mu_{polymer\ chain}$ = 48 TU and $\mu_{polymer\ counterions}$ = 49 TU and by adjusting the resulting curve to the experimental point using a multiplying factor to take into account the unknown detector constant, where TU stands for Tiselius unit (1 TU = 10^{-9} $m^2V^{-1}s^{-1}$). It is worth noting that the effective charged per charged repeating unit can be experimentally determined by capillary isotachophoresis [38, 39] and followed the Manning counterion condensation theory for linear polyelectrolytes.

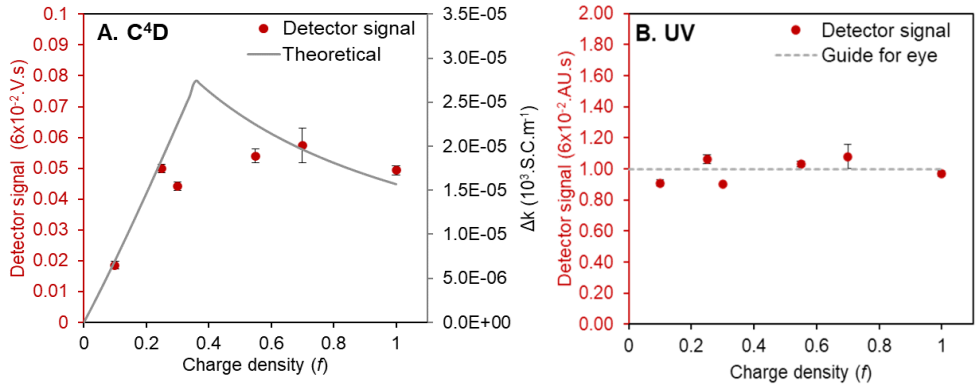

Fig. 5. Variation of experimental detection signal (peak area) of the SPAM family according to the chemical charge density f in C^4D (A) and UV (B). Experimental conditions: fused silica capillary of 60 cm total length (46.4 cm to C^4D detector, 51.5 cm to UV detector) x 50 µm i.d. Eluent: 10 mM MOPS (pH 7.2, ionic strength 5.0 mM, conductivity 355 µS cm^{-1}). Mobilization pressure: 100 mbar. Capillary preconditioning: flushing DI for 2 min followed by BGE for 3 min. Injection: 20 mbar, 10 s (0.6% of the capillary volume to the detector). Sample concentration: 3.0 g L^{-1} in the eluent. UV detection at 200 nm at 25ºC. C^4D parameters: frequency: 2x high, voltage: 0 dB, gain: 50%, offset: 25, baseline value: 565. The plain line in Fig. 5A represents the theoretical C^4D response at constant polymer mass concentration as given by equations (8) and (9) with a floating constant.

All the taylorgrams used to build Fig. 5 are presented in Fig. SI-3. They were fitted with multi-gaussian functions (up to 3), and subtracted from the small ion contribution before integration on the left part of the taylorgram to calculate R_h and *D.* Results are gathered in Table SI-3. The R_h values from C^4D detection were generally lower than the R_h values obtained by UV detection. To better understand these discrepancies, the influence of the polymer molar mass on the C^4D detection response were further studied.

3.4 Studying the effect of molar mass on the sensitivity of detection

Different polyelectrolytes (PLL, APAM and SPAM) with different molar masses were studied to compare the sensitivities of detection in UV and C^4D, as calculated from the slope of the calibration curves (i.e. peak area *vs* concentration). Fig. 6A shows that the sensitivity of detection of the PLL family (molar mass *M* between 3.3 x 10^3 and 6.4 x 10^4 g mol^{-1}) behave very similarly for C^4D and UV detection modes and remains almost constant on the whole range of molar mass. For APAM and SPAM families (see Fig. 6B), the sensitivity of C^4D detection tends to decrease for the highest molar masses, while it was relatively constant in UV detection mode on the entire molar mass range. This tendency observed only for C^4D detection can explain why lower average R_h values were obtained compared to UV, especially for the higher molar mass polymer samples. A possible explanation for this difference in behaviour between UV and C^4D detection could be a drop in the effective mobility of the polymer chain with increasing molar mass of the polymer. Indeed, it is well-known in CE that the effective electrophoretic mobility of synthetic polyelectrolytes decreases with increasing concentration of sieving (entangled or unentangled) polymer solution [40]. Different regimes do exist depending on the molar mass and polymer concentrations, but even in unentangled polymer solutions, transient entanglement or collisions between polymer chains tend to decrease the electrophoretic mobility [41, 42]. The same effect is expected to occur inside the polyelectrolyte zone in TDA, even in absence of sieving matrix, above a certain molar mass and/or injected concentration. And this effect should be more pronounced for higher molar mass polyelectrolytes due to closer entanglements between chains. In UV, since the detection mode does not depend on the effective mobility of the polymer, this phenomenon has no effect on the sensitivity of detection.

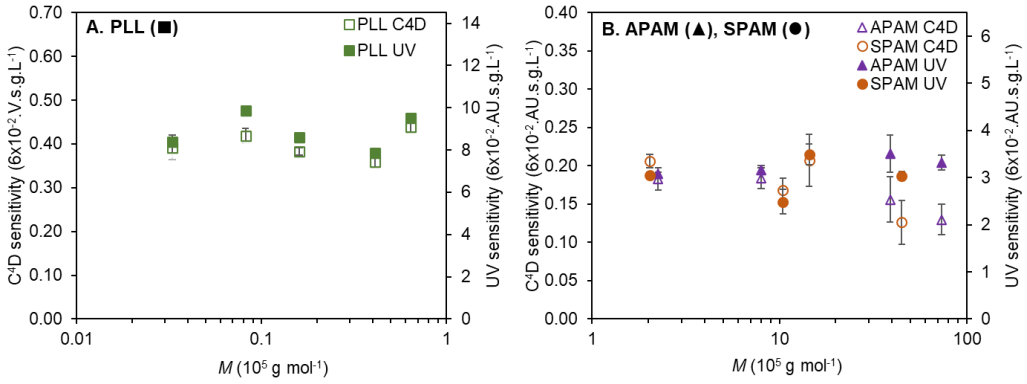

Fig. 6. Variation of detection sensitivity of PLL (A) and APAM or SPAM (B) according to the molar mass (*M*) in C^4D and UV detection. Experimental conditions: for PLL; 0.2% wt PDADMAC coated capillary, for APAM and SPAM; bare-fused silica capillary, 60 cm total length (46.4 cm to C^4D detector, 51.5 cm

to UV detector) x 50 µm i.d. Eluent: for PLL; 8 mM Tris-Cl buffer (pH 7.40, ionic strength 6.7 mM, conductivity 661 µS cm^{-1}), for APAM and SPAM; 10 mM MOPS (pH 7.2, ionic strength 5.0 mM, conductivity 355 µS cm^{-1}). Mobilization pressure: 30 mbar. Injection: 20 mbar, 10 s (0.6% of the capillary volume to the closest detector). Polymer sample: 3.0 g L^{-1} in the eluent. Capillary preconditioning: flushing with water for 2 min followed by BGE for 3 min. UV detection at 200 nm at 25ºC. C^4D parameters: frequency: 2x high, voltage: 0 dB, gain: 50%, offset: 35, 25 and 25 for PLL and APAM, SPAM, respectively. Error bars are +/- SD on n = 5 repetitions.

The taylorgrams of PLL, APAM and SPAM families at the different molar masses with both detectors are shown in Fig. SI-4. The taylorgrams were integrated on their left part after subtraction of the small ions contribution to calculate R_h and D (results in Table SI-2). It was found, for the PLL family (3,300 - 64,000 g mol^{-1}), that the UV and C^4D detectors give similar average R_h values. For the APAM and SPAM family (3 - 9 x 10^5 g mol^{-1}), the UV detector systematically gave higher average R_h values compared to the C^4D detector. Fig. 7 presents a correlation plot between log R_h and log M for the two detection modes and the three families of polyelectrolytes. Using UV detection (plain symbols), we obtained a good linear correlation (in log-log scale) on the entire range of molar mass for the three polyelectrolyte families, as recently observed, even for ultra-high molar mass APAM (up to 25 x10^6 g mol^{-1}) [43]. Using C^4D detection (open symbols), the linear correlation was only obtained for molar masses up to around 100,000 g mol^{-1}. This difference in behavior between UV and C^4D can be explained by the decrease in detection sensitivity at high molar masses in C^4D, which tends to introduce a bias towards the lowest molar masses.

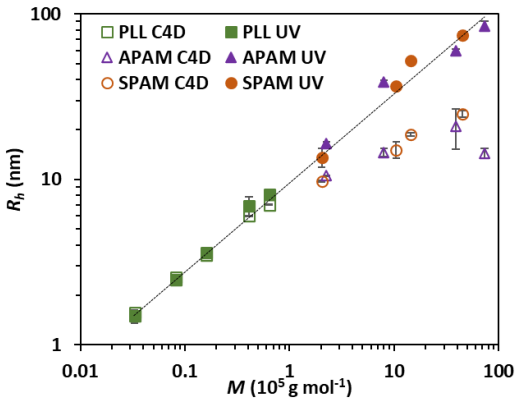

Fig. 7. log R_h – log M plots of both detectors for PLLs, APAMs and SPAMs. Experimental conditions as described in Fig. 6.

3.5 Application of TDA-C^{4}D to non-UV absorbing polyelectrolyte

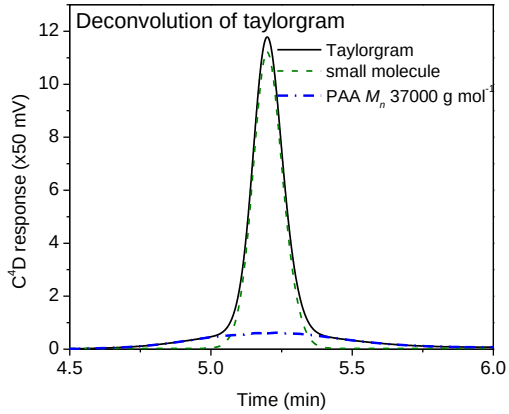

Fig. 8. Taylorgram of PAA M_n = 3.7×10^4 g mol^{-1} and gaussian fit at injected concentrations of 3.0 g L^{-1}. Experimental conditions: fused silica capillary of 60 cm total length (46.4 cm to C^{4}D detector, 51.5 cm to UV detector) x 50 µm i.d. Eluent: 10 mM MOPS sodium (pH 7.2, ionic strength 5.0 mM, conductivity 355 µS cm^{-1}). Injection: 20 mbar, 10 s (0.6% of the capillary volume to the detector). Mobilization pressure: 100 mbar. Capillary preconditioning: flushing with water for 2 min followed by BGE for 3 min. UV detection at 200 nm at 25ºC. C^{4}D parameters: frequency: 2x high, voltage: 0 dB, gain: 50%, offset: 20, baseline value: 565.

As an example of application to non-UV absorbing polymer, poly (acrylic acid) (PAA) was sized by TDA-C^{4}D. The taylorgram of PAA 37000 g mol^{-1} is shown in Fig. 8 before and after subtraction of the small ion contributions. The integration of the polymer contribution leads to R_h = 6.66 ± 0.22 nm (calculated on 4 repetitions at 2 injected concentrations, 3.0 and 5.0 g L^{-1}). This value is in excellent agreement with the R_h value obtained from the intrinsic viscosity $[\eta]$ using eq. (10):

$$R_h = \left(\frac{3[\eta]M}{10\pi \mathrm{N_A}} \right)^{\frac{1}{3}} \qquad (10)$$

where N_A is the Avogadro number and M is the molar mass of the PAA [33]. Eq. (10) gives R_h = 6.88 nm for $[\eta]$ = 222 mL g^{-1} determined on the same PAA sample by capillary viscosity measurements in the same eluent (see Fig. SI-5).

4. Conclusion

In this work, for the first time, TDA has been investigated using a C^{4}D detector. The applied frequency and BGE composition have been studied and optimized. 2x High frequency with 10 mM sodium MOPS pH 7.2 for polyanions, and 8 mM Tris-Cl pH 7.4 for polycation were selected. The effect of polymer chemical charge density on the C^{4}D response was then studied. It was found that the sensitivity of detection in C^{4}D increases linearly with the chemical charge density up to about 37%, and then levels off due to the onset of Manning counterion condensation. The average R_h values provided by the UV and C^{4}D detectors were comparable for low to moderate molar masses polyelectrolytes (M < 10^5 g mol^{-1}). However, for higher molar masses (M > 10^5 g mol^{-1}), the C^{4}D detector provided lower average R_h values compared to UV, probably due to a drop in the electrophoretic mobility of the

polyelectrolyte with increasing molar masses. Therefore, C^4D detection can be an alternative method for sizing low to moderate molar mass charged polymers that do not absorb in UV.

Credit authorship contribution statement

Chutintorn Somnin: Investigation, Writing – original draft. **Joseph Chamieh:** Conceptualization, Supervision, Writing – review & editing. **Phoonthawee Saetear:** Conceptualization, Supervision, Writing – review & editing. **Hervé Cottet:** Conceptualization, Supervision, Writing – review & editing.

Acknowledgements

The authors are grateful for the doctoral scholarship from the Franco-Thai scholarship (Campus France) and the Franco-Thai Mobility Programme/PHC SIAM 2023-2024 supported by Campus France and Ministry of Higher Education, Science, Research and Innovation, Thailand. This project is also funded by National Research Council of Thailand (NRCT) and Mahidol University (Contract # N42A660548). We thank Alexis Guillard and SNF SA (Andrézieux, France) for the gift of the APAM and SPAM copolymer samples.

References

[1] G. Taylor, Dispersion of soluble matter in solvent flowing slowly through a tube, Proc. Math. Phys. Eng. Sci. 219 (1953) 186-203, https://doi.org/10.1098/rspa.1953.0139.

[2] G. Taylor, Conditions under which dispersion of a solute in a stream of solvent can be used to measure molecular diffusion, Proc. Math. Phys. Eng. Sci. 225 (1954) 473-477, https://doi.org/10.1098/rspa.1954.0216.

[3] L. Leclercq, P. Saetear, A. Rolland-Sabaté, J.P. Biron, J. Chamieh, L. Cipelletti, D.J. Bornhop, H. Cottet, Size-based characterization of polysaccharides by taylor dispersion analysis with photochemical oxidation or backscattering interferometry detections, Macromolecules 52 (2019) 4421-4431, https://doi.org/10.1021/acs.macromol.9b00605.

[4] J. Chamieh, J.P. Biron, L. Cipelletti, H. Cottet, Monitoring biopolymer degradation by taylor dispersion analysis, Biomacromolecules 16 (2015) 3945-3951, https://doi.org/10.1021/acs.biomac.5b01260.

[5] F. Oukacine, A. Morel, H. Cottet, Characterization of carboxylated nanolatexes by capillary electrophoresis, Langmuir 27 (2011) 4040-4047, https://doi.org/10.1021/la1048562.

[6] A. Ibrahim, R. Meyrueix, G. Pouliquen, Y.P. Chan, H. Cottet, Size and charge characterization of polymeric drug delivery systems by Taylor dispersion analysis and capillary electrophoresis, Anal. Bioanal. Chem. 405 (2013) 5369-5379, https://doi.org/10.1007/s00216-013-6972-4.

[7] L. Cipelletti, J.P. Biron, M. Martin, H. Cottet, Measuring arbitrary diffusion coefficient distributions of nano-objects by Taylor dispersion analysis, Anal. Chem. 87 (2015) 8489-8496, https://doi.org/10.1021/acs.analchem.5b02053.

[8] H. Cottet, J.P. Biron, M. Martin, Taylor dispersion analysis of mixtures, Anal. Chem. 79 (2007) 9066-9073, https://doi.org/10.1021/ac071018w

[9] P. Saetear, J. Chamieh, M.N. Kammer, T.J. Manuel, J.P. Biron, D.J. Bornhop,H. Cottet, Taylor dispersion analysis of polysaccharides using backscattering interferometry, Anal. Chem. 89 (2017) 6710-6718, https://doi.org/10.1021/acs.analchem.7b00946.

[10] F. Opekar, R. Cabala, T. Kadlecova, A simple contactless impedance probe for determination of ethanol in gasoline, Anal. Chim. Acta. 694 (2011) 57-60, https://doi.org/10.1016/j.aca.2011.03.038.

[11] F. Opekar, P. Tuma, K. Stulik, Contactless impedance sensors and their application to flow measurements, Sensors 13 (2013) 2786-801, https://doi.org/10.3390/s130302786.

[12] F. Opekar, K. Štulík, M. Fišarová, A contactless impedance probe for simple and rapid determination of the ratio of liquids with different permittivities in binary mixtures, Electroanalysis 21 (2009) 96-100, https://doi.org/10.1002/elan.200804366.

[13] D. Shen, D. Li, X. Yang, Y. Zhu, J. Dong, Q. Kang, Application of a low impedance contactless conductometric detector for the determination of inorganic cations in capillary monolithic column chromatography, Talanta 84 (2011) 42-48, https://doi.org/10.1016/j.talanta.2010.12.010.

[14] E. Pungor, F. Pál, K. Tóth, Oscillometric flow cell for measurement of conductivity and permittivity, Anal. Chem. 55 (1983) 1728-1731, https://doi.org/10.1021/ac00261a020.

[15] J.A. Fracassi da Silva, C.L. do Lago, An oscillometric detector for capillary electrophoresis, Anal. Chem. 70 (1998) 4339-4343, https://doi.org/10.1021/ac980185g.

[16] F. Pal, E. Pungor, Oscillometric detector for ion chromatography: A note on detection limit and detector sensitivity. Anal. Chem. 60 (1988) 2254-2258, https://doi.org/10.1021/ac00171a019.

[17] J.A. Fracassi da Silva, C.L. do Lago, Conductivity detection of aliphatic alcohols in micellar electrokinetic chromatography using an oscillometric detector, Electrophoresis 21 (2000) 1405-1408, https://doi.org/10.1002/(SICI)1522-2683(20000401)21:7<1405::AID-ELPS1405>3.0.CO;2-O

[18] W. Huang, B. Chouhan, P.K. Dasgupta, Capillary scale admittance and conductance detection, Anal. Chem. 90 (2018) 14561-14568, https://doi.org/10.1021/acs.analchem.8b04561.

[19] M. Zhang, B.N. Stamos, N. Amornthammarong, P.K. Dasgupta, Capillary scale admittance detection, Anal. Chem. 86 (2014) 11538-11546, https://doi.org/10.1021/ac503245a.

[20] M. Zhang, B.N. Stamos, P.K. Dasgupta, Admittance detector for high impedance systems: design and applications, Anal. Chem. 86 (2014) 11547-11553, https://doi.org/10.1021/ac503247g.

[21] A.J. Zemann, E. Schnell, D. Volgger, G.K. Bonn, Contactless conductivity detection for capillary electrophoresis, Anal. Chem. 70 (1998) 563-567, https://doi.org/10.1021/ac9707592.

[22] P. Kubáň, P.C. Hauser, 20th anniversary of axial capacitively coupled contactless conductivity detection in capillary electrophoresis, Trends Analyt. Chem. 102 (2018) 311-321, https://doi.org/10.1016/j.trac.2018.03.007.

[23] P. Coufal, J. Zuska, T. van de Goor, V. Smith, B. Gas, Separation of twenty underivatized essential amino acids by capillary zone electrophoresis with contactless conductivity detection, Electrophoresis 24 (2003) 671-677, https://doi.org/0173-0835/03/0402–671 $17.50I.50/0.

[24] P. Tůma, B. Sommerová, M. Šiklová, Monitoring of adipose tissue metabolism using microdialysis and capillary electrophoresis with contactless conductivity detection, Talanta 192 (2019) 380-386, https://doi.org/10.1016/j.talanta.2018.09.076.

[25] N. Anik, M. Airiau, M.P. Labeau, C.T. Vuong, H. Cottet, Characterization of cationic copolymers by capillary electrophoresis using indirect UV detection and contactless conductivity detection, J. Chromatogr. A. 1219 (2012) 188-194, https://doi.org/10.1016/j.chroma.2011.11.014.

[26] W.C. Knol, B.W.J. Pirok, R.A.H. Peters, Detection challenges in quantitative polymer analysis by liquid chromatography, J. Sep. Sci. 44 (2021) 63-87, https://doi.org/10.1002/jssc.202000768.

[27] K.A. Oudhoff, M. Macka, P.R. Haddad, P.J. Schoenmakers, W.T. Kok, Contactless conductivity detection of synthetic polymers in non-aqueous size-exclusion electrokinetic chromatography, J. Chromatogr. A. 1068 (2005) 183-187, https://doi.org/10.1016/j.chroma.2004.11.081.

[28] A.J. Zemann, Capacitively coupled contactless conductivity detection in capillary electrophoresis, Electrophoresis 24 (2003) 2125-2137, https://doi.org/10.1002/elps.200305476.

[29] P. Kuban, P.C. Hauser, Fundamental aspects of contactless conductivity detection for capillary electrophoresis Part I: Frequency behavior and cell geometry, Electrophoresis 25 (2004) 3387-3397, https://doi.org/10.1002/elps.200406059.

[30] P. Kuban, P.C. Hauser, Fundamental aspects of contactless conductivity detection for capillary electrophoresis Part II: Signal-to-noise ratio and stray capacitance, Electrophoresis 25 (2004) 3398-33405, https://doi.org/10.1002/elps.200406060.

[31] J.G.A. Brito-Neto, J.A. Fracassi da Silva, L. Blanes, C.L. do Lago, Understanding capacitively coupled contactless conductivity detection in capillary and microchip electrophoresis Part 2. peak shape, stray capacitance, noise, and actual electronics, Electroanalysis 17 (2005) 1207-1214, https://doi.org/10.1002/elan.200503238.

[32] J.G.A. Brito-Neto, J.A. Fracassi da Silva, L. Blanes, C.L. do Lago, Understanding capacitively coupled contactless conductivity detection in capillary and microchip electrophoresis Part 1. fundamentals, Electroanalysis 17 (2005) 1198-1206, https://doi.org/10.1002/elan.200503237.

[33] X. Jin, L. Leclercq, N. Sisavath, H. Cottet, Investigating the influence of phosphate ions on poly(l-lysine) conformations by Taylor dispersion analysis, Macromolecules 47 (2014) 5320-5327, https://doi.org/10.1021/ma501058v.

[34] H. Cottet, J.P. Biron, M. Martin, On the optimization of operating conditions for Taylor dispersion analysis of mixtures, Analyst 139 (2014) 3552-3562, https://doi.org/10.1039/c4an00192c.

[35] Z. Hoherčáková, F. Opekar, A contactless conductivity detection cell for flow injection analysis: determination of total inorganic carbon, Anal. Chim. Acta. 551 (2005) 132-136, https://doi.org/10.1016/j.aca.2005.07.029.

[36] Z. Hoherčáková, F. Opekar, K. Štulík, Thinly insulated wire cells - a new device for sensitive contactless conductivity detection in flow analyses, Electroanalysis 17 (2005) 1924-1930, https://doi.org/10.1002/elan.200503305.

[37] G.S. Manning, Counterion binding in polyelectrolyte theory, Acc. Chem. Res. 12 (1979) 443-449, https://doi.org/10.1021/ar50144a004.

[38] A. Ibrahim, D. Koval, V. Kašička, C. Faye, H. Cottet, Effective charge determination of dendrigraft poly-l-lysine by capillary isotachophoresis, Macromolecules 46 (2013) 533-540, https://doi.org/10.1021/ma302125f.

[39] J. Chamieh, D. Koval, A. Besson, V. Kašička, H. Cottet, Generalized polymer effective charge measurement by capillary isotachophoresis, J. Chromatogr. A 1370 (2014), 255-262, https://doi.org/10.1016/j.chroma.2014.10.025.

[40] H. Cottet, P. Gareil, Electrophoretic behaviour of fully sulfonated polystyrenes in capillaries filled with entangled polymer solutions, J. Chromatogr. A. 772 (1997) 369-384, https://doi.org/10.1016/S0021-9673(96)01057-6.

[41] A.E. Barron, H.W. Blanch, D.S. Soane, A transient entanglement coupling mechanism for DNA separation by capillary electrophoresis in ultradilute polymer-solutions, Electrophoresis 15 (1994) 597-615, https://doi.org/10.1002/elps.1150150184.

[42] A.E. Barron, D.S. Soane, H.W. Blanch, Capillary electrophoresis of DNA in uncross-linked polymer solutions, J. Chromatogr. A. 652 (1993) 3-16, https://doi.org/10.1016/0021-9673 (93)80639-P.

[43] X. Leclercq, L. Leclercq, A. Guillard, L. Rodriguez, O. Braun, C. Favero, H. Cottet, Determination of ultrahigh molar mass of polyelectrolytes by Taylor dispersion analysis, J. Chromatogr. A, 1670 (2022) 462949, https://doi.org/ 10.1016/j.chroma.2022.462949.

Graphical Abstract

Taylor Dispersion Analysis Using Capacitively Coupled Contactless Conductivity Detector

Chutintorn Somnin[1], Joseph Chamieh[1], Phoonthawee Saetear[2,3*], Hervé Cottet[1*]

[1] IBMM, Université de Montpellier, CNRS, ENSCM, Montpellier, France

[2] Flow Innovation-Research for Science and Technology Laboratories (Firstlabs), Ratchathewi District, Bangkok 10110, Thailand

[3] Department of Chemistry and Center of Excellence for Innovation in Chemistry, Faculty of Science, Mahidol University, Rama 6 Road, Ratchathewi District, Bangkok 10400, Thailand

*E-mail address's corresponding authors: herve.cottet@umontpellier.fr (Prof. H.Cottet); phoonthawee.sae@mahidol.edu (Asst. Prof. Phoonthawee Saetear)